Docket No.: 06670/0200961-US0
(PATENT)

IN THE UNITED STATES PATENT AND TRADEMARK OFFICE

In re Patent Application of:
Joshua E. Rothenberg

Application No.: 10/789,374 Confirmation No.: 5126

Filed: February 27, 2004 Art Unit: 2883

For: APODIZED FIBER BRAGG GRATING AND IMPROVED PHASE MASK, METHOD AND SYSTEM FOR MAKING THE SAME

Examiner: C. Y. Peng

CLAIM FOR PRIORITY AND SUBMISSION OF DOCUMENTS

Commissioner for Patents
P.O. Box 1450
Alexandria, VA 22313-1450

Dear Sir:

Applicant hereby claims priority under 35 U.S.C. 119 based on the following prior foreign application filed in the following foreign country on the date indicated:

Country	Application No.	Date
Canada	2,420,521	February 27, 2003

In support of this claim, a certified copy of the said original foreign application is filed herewith.

Dated: April 24, 2006

Respectfully submitted,

By _____

S. Peter Ludwig
Registration No.: 25,351
DARBY & DARBY P.C.
P.O. Box 5257
New York, New York 10150-5257
(212) 527-7700
(212) 527-7701 (Fax)
Attorneys/Agents For Applicant

Office de la propriété intellectuelle du Canada

Un organisme d'Industrie Canada

Canadian Intellectual Property Office

An Agency of Industry Canada

Bureau canadien des brevets

Certification

Canadian Patent Office

Certification

La présente atteste que les documents ci-joints, dont la liste figure ci-dessous, sont des copies authentiques des documents déposés au Bureau des brevets.

This is to certify that the documents attached hereto and identified below are true copies of the documents on file in the Patent Office.

Specification and Drawings, as originally filed, with Application for Patent Serial No: **CA 2420521**, on February 27, 2003, by **TERAXION INC.**, assignee of Joshua E. Rothenberg, for "Improved Phase Mask and Method for Fabrication of FBGs".

Agent certificateur/Certifying Officer

March 24, 2006

Date

Canada

(CIPO 68)
31-03-04

OPIC CIPO

IMPROVED PHASE MASK AND METHOD FOR FABRICATION OF FBGs

FIELD OF THE INVENTION

The present invention concerns a method of phase mask design and a FBG writing method.

BACKGROUND OF THE INVENTION

Writing an FBG comprises two aspects, phase and amplitude. The phase gives the position of the FBG index fringes relative to the assumed underlying uniform pitch, and the amplitude is the magnitude of the index modulation at any given location in the FBG. Variation of the FBG amplitude is often called apodization, since the ends of the FBG must be softened (apodized, or gradually reduced to zero) in order to avoid undesirable group delay and reflectivity ripples, which would result from an abrupt transition from a nonzero amplitude to zero.

To mathematically describe the FBG, the modulation of the effective index of refraction of the single mode fiber can be written as

$$n(x) = n_{eff}(x) + \Delta n(x)\cos(k_{g0}x + \phi_g(x)) = n_{eff}(x) + \mathrm{Re}\{\Delta n(x)\exp[i(k_{g0}x + \phi_g(x)]\} \qquad (1)$$

where the FBG central k-vector is $k_{g0} = 2\pi/\Lambda_g$ and Λ_g is the central period (or pitch) of the grating in the fiber. This index modulation causes a Bragg reflection band at a desired central wavelength λ_B, which is given by $\lambda_B = 2n_{eff}\Lambda_g$, and where n_{eff} is the effective average (i.e. excluding the rapidly varying index modulation) mode index of the single mode fiber.

n_{eff} can be slowly varying and thus it is written in Eq. (1) as $n_{eff}(x)$. $\Delta n(x)$ is the amplitude of the index modulation (this is the apodization profile), and $\phi_g(x)$ is the residual phase (fringe position relative to the uniform period Λ_g, i.e. 2π of phase corresponds to a fringe position shift equal to the full fringe period Λ_g), and x is the position along the fiber. Note that the phase information $\phi_g(x)$ can be used to 'chirp' the grating, which can be used for dispersion compensation, and also the phase can be used for 'sampling', which produces multiple reflection bands that e.g. can be matched to the standard ITU grid frequencies used in commercial WDM systems. Phase sampling has been described in detail in US patent application 09/757386, entitled "EFFICIENT SAMPLED BRAGG GRATINGS FOR WDM APPLICATIONS".

Several methods have been developed for FBG writing using the side illumination method with a phase mask, as illustrated in Fig. 1.

A scanning mechanism is used to illuminate a long section of fiber through the mask, typically with a beam of small diameter (a few mm or smaller). Alternatively, one can scan the mask/fiber pair and keep the writing beam fixed, or avoid scanning entirely and use a writing beam large enough to expose the entire section of fiber required. The mask has a periodic corrugation structure on the surface closest to the fiber, which, when illuminated by the writing laser (typically UV, but not required to be so), generates diffracted orders which transmit an intensity fringe pattern to the FBG. One can write the height (with peaks/valleys of ±d) of the mask surface profile as

$$h(x) = d\sin(k_{m0}x + \theta_m(x)), \qquad (2)$$

where the mask has an underlying period Λ_m and k-vector $k_{m0} \equiv 2\pi/\Lambda_m$, and the residual phase of the mask corrugation function is $\theta_m(x)$. Although we assume a sinusoid here for

simplicity, typically the corrugation of the mask will be closer to a square wave, but this shape does not affect the concept here. The surface grating in the mask causes the writing beam to diffract into multiple orders. The corrugation depth $2d$ is chosen such that the $\pm 1^{st}$ orders are maximized and the 0^{th} order is minimized. Typically this depth will be near the size of the UV wavelength (e.g. $2d \sim 250$ nm). For a uniform mask of period Λ_m, the two 1^{st} order beams will interfere to produce an intensity pattern with a fringe period (and thus the period of the grating in the fiber) $\Lambda_g = \Lambda_m / 2$. In the Prior Art, the mask could be patterned with a nonuniform period (chirp) or phase to produce a similarly varying chirp or phase in the FBG. Thus, the mask could embody the required phase information. However, typically the amplitude information (apodization) was introduced in the writing process itself. The simplest method was simply to vary the laser beam power during writing. However, this method causes a variation in $n_{eff}(x)$, which leads to severe distortion of the FBG reflection spectrum. To correct this a second pass of fiber exposure was used to equalize $n_{eff}(x)$ over the FBG length, but this is more complex and is subject to various uniformity and alignment issues.

A standard technique to achieve apodization without variation of laser power is by controlled wiggling of the mask during writing (see for example Cole et al, US Pat. #6072926). If one wiggles the mask by a distance more than one fringe period the fringes can wash out completely. By changing the wiggling amplitude one can control the net fringe amplitude and thus control the index modulation amplitude $\Delta n(x)$. However, this method is still mechanically complex and is subject to the variations of the mechanical wiggling system. In the absence of such a wiggling apparatus, the mask and the fiber can be mechanically joined by a very simple jig (perhaps just a spacer between the fiber and mask and a clamp to hold them together). This type of mechanical arrangement is likely to have the best thermal and mechanical stability, which can greatly improve the quality of the written FBGs. In addition, as a result of nonlinear writing sensitivity, this method can still have the undesired effect of varying the effective average index $n_{eff}(x)$, distorting the FBG spectrum.

Ideally one would like to include the apodization information in the mask itself, so that the writing process would simply consist of scanning the mask-fiber with the writing laser beam, without additional mechanical variations, or a simple exposure by a stationary large beam.

A few methods have been proposed to incorporate the amplitude information into the mask. One approach uses modulation of the duty cycle (i.e. width), or etch depth, of the grating corrugation on the mask to modulate the intensity of the $\pm 1^{st}$ and 0^{th} order diffracted beams, such that the visibility of the fringes in the transmitted light is varied. This approach suffers from a number of practical difficulties in achieving the desired flexibility and accuracy of the amplitude profile, and since the visibility of the fringes is modulated, it is possible that it could generate some undesirable variation of the effective average index of the fiber core, $n_{eff}(x)$. A summary of these prior art methods can be found in the book by Kashyap (Fiber Bragg Gratings).

Using interference between two FBG fringe patterns to control fringe amplitude, is disclosed in Kashyap, U.S. Patent No. 6,307,679. However, the two component FBG patterns are written sequentially. As a result, the prior art method disclosed in Kashyap suffers from the problem that the longitudinal position of the fiber must remain very precisely controlled, generally on the scale of 1 nm, between the sequential writing passes of the two FBG patterns. In addition, the writing laser power and beam position and angle must be very precisely maintained between the two writing passes. A number of approaches were recently proposed in a US patent application (Popelek et al, "Embodying Amplitude Information into Phase Masks," US application no. 10/154,505, filed 5/24/02) which used a single illumination of the combination of multiple patterns on the same mask to achieve the required apodization.

Therefore there is a need for an improved phase mask and a FBG writing method overcoming the drawbacks of the prior art methods discussed therein.

SUMMARY OF THE INVENTION

The present invention enables the use of extremely precise phase-only variations (i.e. the positions of the individual grooves) in a phase mask design to achieve apodization that would otherwise require modulation of the fringe depth in an FBG. This approach has significant advantages over the prior art. First, it allows for fabrication of complex FBGs with a very simple exposure, without for example, the need to use a very small scanned writing beam, or the use of complex mechanical systems such as needed for piezo-driven dithering. (The exposure could be just a blanket illumination with a stationary large beam). Second, this method of apodization has reduced, if not zero, side effects on varying the average index of the FBG – a problem that can occur with other methods. Finally, the method has high resolution and mathematical precision, leveraging the precision of semiconductor lithography tools. This enables the manufacture of high resolution and complex FBGs using a precise mask and an extremely simple exposure procedure.

Other advantages of the present invention will be better understood upon reading preferred embodiments thereof with reference to the appended drawings.

BRIEF DESCRIPTION OF THE DRAWINGS

The present invention will be described in more detail below with references to the accompanying drawings in which:

Figure 1 is a schematic representation of prior art standard method for writing an FBG by side illumination through a phase mask.

Figure 2 is a graph illustrating the effective relative modulation amplitude of FBG fringes resulting from phase only apodization with sinusoidal phase versus the amplitude of the sinusoid according to a preferred embodiment of the present invention.

Figure 2(b) is a graph illustrating the transfer amplitude of sinusoidal phase vs spatial frequency according to a preferred embodiment of the present invention.

Figure 3 shows graphic representations of a phase-only apodization of a single channel linearly chirped grating according to another preferred embodiment of the present invention.

Figure 4A shows graphic representations of a phase-only apodization of the same linearly chirped FBG as in Fig. 3; the apodization period being 200 μm.

Figure 4B shows graphic representations of experimental results of Phase-only apodization of a linearly chirped single channel FBG; the apodization period being about 24 μm.

Figure 4C shows graphic representations of experimental results of Phase-only apodization of a linearly-chirped single channel FBG, according to another preferred embodiment of the present invention.

Figure 5 shows graphic representations of Phase-only apodization of a nonlinearly chirped FBG, according to another preferred embodiment of the present invention.

Figure 6 shows graphic representations of Phase-only apodization of another nonlinearly chirped FBG, according to another preferred embodiment of the present invention.

Figure 7 shows graphic representations of Phase-only apodization of another nonlinearly chirped FBG, according to another preferred embodiment of the present invention.

Figure 8 shows graphic representations of a 9-channel phase-only sampling FBG. The top panel shows the periodic phase, which generates the uniform 9 central channels while the bottom panel shows the spectral *amplitude* of the channels generated by the sampling.

Figure 9 shows graphic representations of the spectrum of a 9-channel phase-only sampling of Figure 8, which has been modified to include phase-only apodization , according to another preferred embodiment of the present invention.

Figure 10 shows graphic representations of the spectrum of a 9 channel phase-only sampling FBG, which has been modified to include phase-only sinusoidal apodization, according to another preferred embodiment of the present invention.

Figure 11 shows graphic representations of the spectrum of 41-channel FBG with phase-only sampling and apodization, according to another preferred embodiment of the present invention.

Figure 12 shows graphic representations of a 9 channel linearly chirped phase-only sampled FBG, which has been phase-only apodized, according to another preferred embodiment of the present invention.

Figure 13 shows graphic representations of a central channel of 9-channel linearly chirped phase-only sampled FBG, which has been phase-only apodized.

Figure 14 shows graphic representations of a 41 channel linearly chirped phase-only sampled FBG, which has been phase-only apodized, according to another preferred embodiment of the present invention.

Figure 15 shows graphic representations of the central channels of 41-channel linearly chirped phase-only sampled FBG, which has been phase-only apodized.

While the invention will be described in conjunction with an example embodiment, it will be understood that it is not intended to limit the scope of the invention to such embodiment. On the contrary, it is intended to cover all alternatives, modifications and equivalents as may be included as defined by the present description.

DESCRIPTION OF PREFERRED EMBODIMENTS OF THE INVENTION

In this disclosure a new method of incorporating amplitude information into a *single* pattern in the mask is described. In the proposed method the amplitude of the grating is varied by including an additional variation into the location (i.e. phase) of the corrugations on the mask. This additional phase variation causes the amplitude of the grating in the FBG, near the central period of interest Λ_g, to vary in a precise way. As opposed to the prior art methods that vary the diffraction efficiency into the 0^{th} and 1^{st} orders, this method redistributes angularly the UV

light within the 1st order in such a way as to vary the amplitude of the grating near the period of interest, while introducing additional fringes that have a period outside of the region of interest. In this way, one can effectively achieve apodization of the index fringes *relevant to the spectral region of interest*, while the actual total fringe amplitude $\Delta n(x)$ is completely constant. Therefore, one substantially eliminates any potential variation in the average index $n_{eff}(x)$, which can result from nonlinear writing sensitivity.

Referring to Eq. (1), the essential idea here is to replace the amplitude function $\Delta n(x)$ by a phase only function. Thus define a 'phase apodization' function

$$A(x) = \Delta n_0 \exp[i\phi_{AP}(x)] \tag{3}$$

One sees that the function $A(x)$ has a completely uniform amplitude Δn_0, and thus is entirely defined by the apodization phase function $\phi_{AP}(x)$. The goal will be to design $A(x)$ such that it can replace $\Delta n(x)$ in Eq. (1) and the resulting FBG spectrum will achieve the desired performance required for the device *in the spectral region of interest*. Thus the index modulation in the fiber core is written as

$$n(x) = n_{eff} + \mathrm{Re}\{A(x)\exp[i(k_{g0}x + \phi_g(x)]\} = n_{eff} + \Delta n_0 \,\mathrm{Re}\{\exp[i(k_{g0}x + \phi_g(x) + \phi_{AP}(x)]\} \tag{4}$$

From equation (4) one sees that the index modulation is now a constant Δn_0 and has no amplitude variation whatsoever. The FBG could then be written with an appropriate phase mask that incorporates both the usual designed grating phase $\phi_g(x)$ (e.g. chirp etc) and the proposed apodization phase $\phi_{AP}(x)$, and thereby no modulation of the actual fringe amplitude would be required, either through wiggling of the phase mask or by other methods.

To understand the basic proposal it is helpful to realize that for FBGs with small index modulation, the reflection spectrum of the grating can be found from the Fourier Transform of the complex index modulation function (the quantities for which the Real part is taken in Eqs. (1) and (4)). As was disclosed in US applications 10/056,575 and 09/757,386, Fourier analysis can be valid even for large index modulation. The application of Fourier analysis here is directed at understanding the effect of small scale-length periodic phase modulation on the grating spectrum. If the reflectivity developed over this scale-length is small, then generally the Fourier theory can be applied to understand the distribution of the spectrum among many channels generated by the periodic phase modulation even for highly reflecting gratings. It should be understood that the Fourier analysis used here is illustrative only, and the invention is not dependent on Fourier design.

Note that reflection from any point in the FBG will correspond to a delay time given by the round trip time from the entrance of the FBG to the point of reflection $\tau = 2n_g x/c$, where n_g is the effective group index of the fiber. Thus the reflection spectrum, relative to the center frequency of the grating $\nu_0 = c/\lambda_B = c/2n_{eff}\Lambda_g$, can be written as

$$R(\Delta\nu) \propto \left| \Im\{\exp[i(\phi_g(x) + \phi_{AP}(x))]\}_{f=2n_g\Delta\nu/c} \right|^2 \qquad (5)$$

where $\Delta\nu = \nu - \nu_0$, and f is the Fourier transform spatial frequency variable corresponding to the x-position along the fiber. Thus, for example, if the grating phase has a period P, then the Fourier transform will have peaks at spatial frequency $f = 1/P$ and its harmonics $f = m/P$, and thus the reflectivity will have peaks (or channels) at harmonics $\Delta\nu = mc/2n_g P$, where m is an integer. As an example, if P = 100 μm, then the channel spacing Δν ~ 1000 GHz ~ 8 nm.

The basic idea that is proposed here is to set $\phi_{AP}(x)$ equal to a rapidly varying sinusoid (although it is not limited to a sinusoid, the sinusoid is a particularly simple embodiment to analyze) whose amplitude is slowly varying (in comparison to the period of the sinusoid) as a function of x. The result, in effect, will be that this sinusoidal phase variation causes the FBG fringes to (partially or completely) disappear *in the spectral region of interest* while generating spurious fringes at a period well out of the spectral range of interest. Put another way, as described above, a periodic phase variation will cause generation of harmonic sideband channels in the reflection spectra. These spurious 'apodization' sideband channels are generated at the expense of reducing the reflection response in the central channel of interest. That is, the sinusoidal phase modulation effectively reduces the reflectivity in the central channel, or equivalently reduces the effective amplitude of the grating responsible for the reflectivity of the central channel. If this apodization phase variation has a period P_A, then according to the discussion above, spurious reflectivity 'channels' will be created at a frequency separation from the center channel(s) of interest of $\Delta\nu_{AP} = mc/2n_g P_A$, where m is an integer. If we make P_A small enough, then these channels will be far out of the spectral region of concern. For example, the telecommunications C-Band is roughly 4 THz wide. So if P_A is less than ~ 25 μm then the separation of these spurious 'apodization' side bands will be more than 4 THz, and these sidebands will therefore be in a spectral region which is unimportant and could be ignored.

Thus, one defines the apodization phase as

$$\phi_{AP}(x) = \phi_0(x)\sin(2\pi x/P_A) \tag{6}$$

where the amplitude of the sinusoid $\phi_0(x)$ varies slowly in comparison to the sinusoid period P_A. To understand how this method works first consider this phase apodization as used with a uniform grating of wavenumber k_{g0}. That is, let the FBG modulation be given by

$$n(x) = n_{eff} + \Delta n_0 \,\mathrm{Re}\{\exp[i(k_{g0}x + \phi_{AP}(x)]\} \tag{7}$$

From Eq. (5) it is seen that the reflectivity is given by

$$\begin{aligned} R(\Delta\nu) &\propto \left|\Im\{\exp[i\phi_{AP}(x)]\}\right|^2_{f=2n_g\Delta\nu/c} \\ &= \left|\Im\{\exp[i\phi_0(x)\sin(2\pi x/P_A)]\}\right|^2_{f=2n_g\Delta\nu/c} \end{aligned} \tag{8}$$

Now one makes use of the identity

$$\exp[i\phi_0\sin(\theta)] = \sum_{m=-\infty}^{\infty} J_m(\phi_0)\exp[im\theta] \tag{9}$$

where J_m is an ordinary Bessel function. One takes $\theta = 2\pi x / P_A$ and assumes $\phi_0(x)$ is slowly varying and can be treated as a constant to obtain

$$R(\Delta\nu) \propto \left|\Im\left\{\sum_{m=-\infty}^{\infty} J_m(\phi_0)\exp[im2\pi x/P_A]\right\}\right|^2_{f=2n_g\Delta\nu/c} \tag{10}$$

Thus, one sees the reflectivity consists of a series of channels, and one assumes only the central channel ($m = 0$) is in a spectral region which is of interest and therefore the spurious 'apodization channels' ($m \neq 0$) can be ignored. This leaves a central channel as would be reflected by a uniform grating with an equivalent amplitude given by the coefficient $J_0(\phi_0)$. Therefore if $\phi_0(x)$ is slowly varying in comparison to the apodization period P_A, then the effective amplitude of the central channel grating varies as a function of the position x along the fiber according to the relationship

$$\Delta n(x) = \Delta n_0 J_0(\phi_0(x)) \tag{11}$$

or $$\phi_0(x) = J_0^{-1}(\Delta n(x)/\Delta n_0) \quad (12)$$

where Δn_0 is the maximum grating amplitude when the phase apodization ϕ_0 is zero. Thus, the effective reduction in $\Delta n/\Delta n_0$ is given by the 0^{th} order Bessel function J_0, which is plotted in Fig. 2. One sees that the reduction of Δn varies smoothly with ϕ_0 until Δn reaches zero at the first zero of J_0 at $\phi_0 = 2.4048$. Thus one can fully control the apodization by designing $\phi_0(x)$ to precisely vary between 0 and 2.4048.

To summarize the basic idea more concisely, if one desires to write the grating with index modulation

$$n(x) = n_{eff} + \mathrm{Re}\{\Delta n(x)\exp[i(k_{g0}x + \phi_g(x)]\} \quad (13)$$

one can instead write a grating with no amplitude variation along the length $\Delta n(x)$, i.e. a grating with constant fringe amplitude Δn_0 and "phase-only" apodization as in Eq. (4)

$$n(x) = n_{eff} + \Delta n_0\,\mathrm{Re}\{\exp[i(k_{g0}x + \phi_g(x) + \phi_0(x)\sin(2\pi x/P_A)]\} \quad (14)$$

where $\phi_0(x)$ is given by Eq. (12). P_A is required to be sufficiently small such that the spurious sidebands at $\Delta\nu = mc/2n_g P_A$ are of no concern, and that the scale of the variation in $\Delta n(x)$ is long compared with P_A. Note that Eq. (12) is based on the validity of the approximations of FBG reflectivity developed in US patent applications 10/056,575 and 09/757,386. The invention is not dependent on the exact formulation of Eq. (12). For example, one can experimentally measure the values of $\phi_0(x)$ required to obtain a desired level of apodization, and thereby modify Eq. (12) to be calibrated to experimental result.

Alternatively a more sophisticated FBG analysis (e.g. transfer matrix methods) could be used to obtain a more accurate formulation of Eq. (12).

To examine how this method works, one can calculate the performance of the method of Eqs. (14) and (12) on some sample FBG designs. In all of the designs considered here, the conventionally required FBG apodization $\Delta n(x)$ is obtained by Fourier synthesis. However, this is done for simplicity and numerical convenience only. For more complex designs, such as those with high reflectivity spectra, a more sophisticated design method, such as inverse scattering techniques (see e.g. Feced et al. J. Quantum Electron. Vol. 35, p1105-1115, 1999), could be used to determine $\Delta n(x)$. Then, one could apply Eq. (12) (or an appropriately modified form) using $\Delta n(x)$ found by such a design method to obtain $\phi_0(x)$ and generate a phase-only apodized grating as described by Eq. (14). Indeed, any method may be used to design a desired apodization profile $\Delta n(x)$ and then Eq. (12) or a modified version may be used to define a phase-only apodized grating using Eq. (14).

Figure 3 shows the result of phase-only apodization for a simple linearly chirped single channel FBG with 1000 ps/nm dispersion. The period of the apodization sinusoid is chosen to be 200 μm, so that the spurious apodization channels are separated by about 4 nm (500 GHz) from the desired dispersion compensation channel. The first panel shows the desired and effectively achieved apodization profile by varying of $\phi_0(x)$, as determined by Eqs. (11) and (12). The second panel shows the actual amplitude variation assumed for $\Delta n(x)$. One sees in the second panel that $\Delta n(x)$ is taken to be constant over the entire active region of the grating (this is arbitrarily taken to be the length over which the effective amplitude $\Delta n(x)$ is greater than 2×10^{-4} of the peak), but it is reduced to zero at the ends of the region to eliminate spurious reflection that could result from the abrupt change at the end. If suppression of the end reflection is needed, then the transition at the grating ends can be essentially of any form so long as the transition is not too rapid. In the case of Fig. 3, there are no adverse effects for end

transition regions wider than about a few 100 μm. As a result, a number of prior-art techniques could be used to incorporate the end transitions into the mask, since they are not critical. One method is just a gradual reduction of the width or depth of the mask grooves over the transition region. In general, one would expect that for larger spectral separation of the spurious apodization channels, the termination of the grating ends should be less critical. The 'end' apodization is included in the simulations here for numerical convenience only, and is not a required aspect of the invention. However, it is possible that it may be beneficial in some grating designs. As will be noted below, the experimental results indicate that such grating end apodization is not necessary to achieve excellent results (at least for the dispersive grating design used in this measurement).

The third panel shows the calculated group delay (solid) compared to the desired linear variation (dashed), and the fourth panel shows the difference between the desired and calculated delays. The final panel shows the calculated reflectivity *amplitude* of the phase-only apodized grating. One sees that over the ~0.4 nm bandpass of the reflective channel there is no discernable difference between the desired and calculated group delay (i.e. zero group delay ripple), thus demonstrating the phase-only apodization method works as desired.

Figure 4A shows this same calculation on a wide bandwidth scale so that one can observe the spurious 'apodization channels'. One sees that these channels have separation of ~ 4 nm (500 GHz) as one would expect from the apodization period P_A = 200 μm. Note also, as seen in the last panel of Fig. 4A, each of the spurious channels is peaked near its spectral edges, and the response in the center of each spurious channel is near zero. This is simply a result of the redistribution caused by the phase-only apodization method. The apodization does not reduce the reflectivity at the center of the desired channel and so does not induce reflectivity at the center of the spurious channels. However, the apodization does reduce the reflectivity at the edges of the desired channel, by redistributing it at the edges of the spurious channels.

Mathematically, this behavior stems from the fact that the amplitude of the gratings associated with the spurious channels is given by higher order Bessel functions, as seen in Eq. (10).

As mentioned earlier, with $P_A \leq 25$ μm, one would obtain a separation of more than 32 nm, exceeding the entire width of the telecommunications C-band. Such an experimental result, using a phase-only apodized, linearly-chirped FBG of dispersion ~ -1500 ps/nm, is shown in Fig. 4B. The apodization period P_A ~ 24 μm. One sees that the frequency separation of the spurious channels is ~ 4.3 THz (or ~ 35 nm, an interval corresponding to ~ 43 channels separated by 100 GHz). The structure of the spurious channels, as seen in the enlargements of peaks (a) and (c), is exactly as predicted in Fig. 4A, with a minimum at the spurious channel center and the reflectivity peaked near the spurious channel edges. The desired central channel shows a smooth reflectivity with no significant side lobes and the noise floor outside the channel is more than 30 dB down from the peak. The bottom panel of Fig. 4C shows the measured group delay response of the central channel. One observes very small group delay ripple, less than 8 ps peak-to-peak. This is another indication that the apodization method is achieving excellent results. It should be emphasized that this experimental result was obtained without any additional apodization (by means other than the designed phase-only method) of the grating ends whatsoever. This demonstrates that phase-only apodization alone may be used to fabricate dispersion compensating FBGs with excellent spectral characteristics.

Figures 5 and 6 show calculations of phase-only apodization of nonlinearly chirped single channel gratings. The dispersion varies linearly over the channel bandwidth according to $D = (-500\,ps/nm) + (800\,ps/nm^2)\Delta\lambda$ for Fig. 5 and $D = (-30\,ps/nm) + (2000\,ps/nm^2)\Delta\lambda$ in Fig. 6. The plots are similar to those above, but the first panel shows the desired and achieved apodization profiles on a linear scale, whereas the second panel shows the desired apodization (dashed) and actual constant $\Delta n(x)$, with tapers at the ends, on a log scale. The apodization period used in Fig. 5 is 50 μm.

Note that in Fig. 6 the target apodization profile has very dramatic oscillations from maximum to near zero, and thus is a rigorous test of the phase-only apodization method. In the fourth panels one sees again that the group delay is indistinguishable from the desired quadratic over the central portion of the reflectivity channel. The apodization period used in Fig. 6 is 25 μm, but if one increases this period, one starts to observe errors in the calculated spectrum. This effect is shown in Fig. 7, which is the same grating design as in Fig. 6, except that the phase apodization period has been taken as 100 μm. One sees modest but significant group delay error in the channel center as well as amplitude error in the wings of the reflectivity. This appears to result from the rapid oscillations in the desired apodization profile. The phase modulation amplitude $\phi_0(x)$ can no longer be considered to vary slowly over a period P_A of the apodization. Therefore, it can no longer be linked directly to an apodization profile, as indicated in Eq. (11). In order for this interpretation to hold and to properly achieve the target design, the phase apodization is then required to have a shorter period. If the apodization period cannot be reduced, the phase profile $\phi_0(x)$ can be designed with a different approach than prescribed by Eq. (12). For example, a nonlinear optimization iterative process can be used, such as the simulated thermal annealing, simplex, Gerchberg-Saxton, and other optimization methods described in US patent applications 10/056,575 and 09/757,386, whereby the complex reflectivity spectrum is calculated at each iteration and the phase profile $\phi_0(x)$ and/or the underlying grating phase $\phi_G(x)$ is varied until the desired complex reflectivity is achieved to a desired level of accuracy.

As discussed in previous US patent applications 10/056,575 and 09/757,386, a periodic phase included in the grating design can be used to "sample" the FBG and thereby generate a series of periodically spaced channels that can be adapted for use in a commercial WDM system. Figure 8 shows such a periodic phase that has been designed to generate 9 uniform channels (uniformity of 9 central channels is better than 1%, but many unused 'extra' channels are also generated). The phase apodization method may be used in conjunction with the "phase sampling" to reduce the amplitude of all 9 of these channels by adding a periodic phase of

sufficiently high frequency such that the spurious 'apodization channels' are adequately spaced away from the desired central 9 channels and therefore do not cause noticeable interference. Thus one would have an index modulation given by

$$n(x) = n_{eff} + \Delta n_0 \,\mathrm{Re}\{\exp[i(k_{g0}x + \phi_g(x) + \phi_{Samp}(x) + \phi_0(x)\sin(2\pi x / P_A)]\} \qquad (15)$$

where $\phi_{Samp}(x)$ is the periodic sampling phase, and $\phi_g(x)$ is the underlying phase corresponding to the chirp common to all the channels. The period of $\phi_{Samp}(x)$, P_{Samp} determines the spacing of the central channels according to $\Delta\nu_{Samp} = c/2n_g P_{Samp}$. For example, if $P \sim 1.03$ mm, then the channel spacing $\Delta\nu \sim 100$ GHz, a standard ITU spacing for WDM channels. Phase-only apodization of a 9 channel spectrum generated by the phase of Fig. 8 and according to Eq. (15) is demonstrated in Figs. 9-10, where the apodization phase amplitude is applied as per Eq. (12) [ϕ_0=2.386 and 2.4046] so as to reduce the amplitude of the central 9 channels to 10^{-2} and 10^{-4} of the maximum, respectively. The phase apodization is seen to impact equally on all 9 channels. Note that as the amplitude is decreased, the interference from the unwanted channels in the wings generated from the spurious 'apodization channels' becomes more of an issue. This constrains the apodization frequency to be large enough so that this potential overlap is not significant. In this case, the apodization period $P_A \sim 25$ μm corresponds to a 40 channel (at 100 GHz spacing or 4 THz) shift of the apodization channels, which is seen to be adequate to obtain good uniformity of the 9 channels at the 10^{-4} level. As one increases the channel count of the desired central band, then the apodization period will need to be decreased to insure adequate separation between the desired channels and the spurious apodization channels.

For example, Fig. 11 shows a 41 channel phase-only sampled grating apodized to a target level of 10^{-2}. The phase apodization applied is uniform with ϕ_0=2.386 and period P_A = 8.3 μm, corresponding to a ~ 124 channel (12.4 THz) shift of the apodization channels. Because

this shift is insufficient, one observes significant nonuniformity (> 30%) in the amplitude of the center 41 channels, owing to interference from the spurious apodization channels. Simulations (see Figs. 14 and 15) show that a ~154 channel shift (15.4 THz frequency shift or apodization period $P_A \sim 6.7$ μm) is sufficient to achieve adequate uniformity.

In the calculations of Figs. 8-11 $\phi_g(x)$ is taken to be zero and one obtains identical channels each originating from a uniform grating, and thus only the overall channel amplitudes are plotted. If instead $\phi_g(x)$ is chosen to give a linear chirp (i.e. a quadratic phase), then one obtains a multi-channel grating with equal dispersion in each channel. An example of this is shown in Figs. 12-13, where $\phi_g(x)$ is chosen to correspond to a dispersion of $D = 1000$ ps/nm. One sees that 9 uniform channels with identical linear group delay are obtained. The deviation of the group delay from the desired linear design is seen to be negligible in the single channel plot of Fig. 13. Here again the apodization period selected is $P_A = 25$ μm (40 channel shift), which is seen to be adequate to insure good uniformity and negligible group delay ripple in each of the desired channels.

Similar calculations are shown in Figs. 14-15, but in this case the phase-only sampling is designed for 41 central channels. As a result, a much larger offset for the spurious apodization channels is required to avoid interference between channels, and thus undesirable nonuniformity and group delay ripple. Therefore, an apodization period of $P_A \sim 6.7$ μm is used in these calculations, which corresponds to an apodization frequency of ~ 15.4 THz or an offset of ~ 154 channels. From Figs. 14-15 one sees that the apodization with a 15.4 THz offset is sufficient to insure good uniformity and negligible group delay ripple in each of the desired channels.

Practical Implementation of FBG Writing Method

Fabrication of FBGs with complex and high frequency phase patterns using a mask is discussed at length in US patent application 10/056,575 and its disclosure Phaethon memo TM010. A standard arrangement used for FBG side writing, with the fiber proximal to the mask may be utilized. One may scan a writing beam as shown in Fig. 1 (except that the mask wiggling actuator is not included), or a large stationary beam may be used to expose the entire required section of the FBG. It was disclosed there that one must account for the diffraction from the mask to the core of the fiber to properly design the mask to achieve the desired phase variation in the FBG. These diffraction effects are more easily compensated if one minimizes the distance between the mask and the fiber. Here, the essential results are summarized, and the application to the phase-only apodization method is described. It should be understood that this approach is a simple approximation, and that a more sophisticated diffraction analysis (e.g. propagation of plane wave spectra, or vector diffraction) may be needed for some mask-fiber spacings and grating designs.

It is desired to write an FBG with phase for apodization given by Eq. (6)

$$\phi_{AP}(x) = \phi_0(x)\sin(2\pi x f_A) \tag{16}$$

where $f_A = 1/P_A$ is the spatial frequency of the apodization sinusoid. As described in the disclosure TM010, because the $\pm 1^{st}$ order diffracted beams, which interfere to form the FBG, meet the fiber core at a distance Δz away from the mask, and are incident at an angle θ_0 away from normal incidence, they come from slightly displaced positions $x = \pm\Delta x/2$ at the mask, where Δx is defined by the diffraction angle θ_0 and the mask-fiber spacing (see Fig.1 and Eq. 14 of application 10/056,575). If one describes the phase of the mask corrugation by $\theta_m(x)$,

then it was shown in application 10/056,575 that the phase of the grating in the core of the fiber, is given by

$$\phi_{FBG}(x) = \theta_m(x - \Delta x/2) + \theta_m(x + \Delta x/2) \tag{17}$$

Taking the Fourier transform, one obtains the phase frequency transfer function for the mask-to-fiber writing process:

$$\tilde{\phi}_{FBG}(f) = 2\cos(\pi f \Delta x)\tilde{\theta}_m(f) \tag{18}$$

where $\tilde{\phi}_{FBG}$ and $\tilde{\theta}_m$ are Fourier transforms and f is the spatial frequency of the mask or FBG phase. Thus, in the case of apodization with a sinusoidal phase as defined in Eq. (16), one designs the mask to have an apodization phase (in addition to any other phase components designed for chirp or sampling) with a sinusoidal component defined by

$$\theta_{AP}(x) = \theta_{AP0}(x)\sin(2\pi x f_A), \tag{19}$$

where the appropriate mask phase amplitude $\theta_{AP0}(x)$ is designed to account for diffraction, and can be found using Eqs. (16) and (18):

$$\theta_{AP0}(x) = \phi_0(x)/2\cos(\pi f_A \Delta x) \tag{20}$$

To achieve robust manufacturing with this technique, one desires to have a maximum tolerance to changes in the fiber-mask distance. Variations in this distance cause a change in Δx and thus would alter the effective amplitude of the sinusoidal phase. Differentiation of the relationship (20) gives the incremental change in the phase amplitude for an incremental change δx in the value of Δx

$$\delta\phi_0(x) = -2\pi f_A \theta_{AP0}(x)\sin(\pi f_A \Delta x)\delta(\Delta x) \qquad (21)$$

Thus, to achieve the greatest tolerance to changes in Δx one sees that it is desirable to minimize f_A, however this may not be possible since for some designs f_A must be sufficiently large to resolve rapid changes in apodization and to avoid interference from multiple channels. For large f_A, one can still achieve good tolerance by choosing f_A such that the sin in Eq. (21) is zero – i.e. when $f_A \Delta x = m$, an integer. As an example, if the mask-fiber distance is ~ 10 μm, then one finds that $\Delta x \sim 25$ μm, and the sin factor will be zero for f_A = 1/25, 2/25, or 3/25 μm^{-1} etc; or equivalently P_A = 25, 12.5, or 8.3 μm etc (i.e. $P_A = \Delta x / m$). In Fig 2(b) the transfer amplitude (Eq. 18 normalized) is plotted for the case where Δx = 25 μm, and the spatial frequency has been scaled in terms of the frequency shift of the apodization channels in units of 100 GHz intervals (i.e. $(cf_A / 2n_g)/100\,\mathrm{GHz}$). Thus, e.g. an apodization period of P_A = 25 μm would correspond to a shift of ~40, 100 GHz channels. From Fig. 2(b) one sees that the transfer amplitude has extrema at ~ 40, 80, 120, 160 channels. At these extrema one has zero derivative (as per Eq. (21)) and thus maximum tolerance to changes in the mask to fiber distance. However, from inspection of Eqs. (20) and (21), one can see that the higher order extrema at larger f_A still have increased sensitivity to changes in Δx. Thus, one would like to operate at the first extremum (40 channels in this example), yet f_A must still be large enough such that undesirable interference effects do not limit the FBG performance. As shown above, for 40+ channel designs the required value of f_A may be as large as ~ 16 THz (160 channels). In this case one must insure greater mechanical stability such that the changes in Δx are minimized.

The essential suggestion here is to apply a sinusoidal phase modification to the phase mask in order to precisely control the apodization characteristics of the FBG. The phase modification does not necessarily need to be sinusoidal. The Fourier analysis presented here is not a

required aspect of the invention, but included as an example of the analysis that may be used to obtain a satisfactory grating design. The broadest statement of this invention is a method to control the apodization amplitude of the channel(s) of interest by a phase-only modification to the FBG and/or mask. This approach **requires** that the reduction of apodization and reflectivity in the channel(s) of interest **must** be accompanied by a redistribution of reflectivity to another spectral region (which by design should be of no concern).

It should be noted that the analysis of sinusoidal phase apodization and its implementation in the mask is based on the approximate relationship found between the mask and fiber phase and disclosed in US application 10/056,575, as described above in Eqs. (17) and (18). In practice this approximation may be inadequate, especially for higher apodization frequencies, where a more complete diffraction analysis is required. However, regardless of the analytic method, one can always perform an experimental calibration of the effective apodization obtained as a function of the periodic (perhaps sinusoidal) apodization phase amplitude. Such a calibration would then replace the analytic result of Eq. (20), or some more sophisticated diffraction calculation. The experimental calibration curve obtained would then replace Fig. 2, and an empirically calibrated, modified version of Eq. (12) could then be used to design $\phi_0(x)$ and thus the mask for any given desired apodization profile, in a manner similar to that described by Eqs (11) – (14). In addition, the phase modulation for apodization and the phase of the underlying grating design may be optimized to achieve the desired apodization and FBG spectral response by a number of well known techniques, such as those described to optimize the sampling spectrum in US applications 10/056,575 and 09/757,386.

It may also be beneficial to combine the proposed technique with prior art concepts such as variation of the mask groove depth or width along the length of the grating. This approach may be helpful at the very ends of the grating, where some type of amplitude apodization may be helpful in avoiding spurious FBG reflections owing to the abrupt end of the phase apodization. It should be emphasized that apodization of the grating ends by a means other

than phase-only apodization is not a required aspect of the invention, but may be beneficial in some circumstances.

Although preferred embodiments of the present invention have been described in detail herein and illustrated in the accompanying drawings, it is to be understood that the invention is not limited to these precise embodiments and that various changes and modifications may be effected therein without departing from the scope or spirit of the present invention.

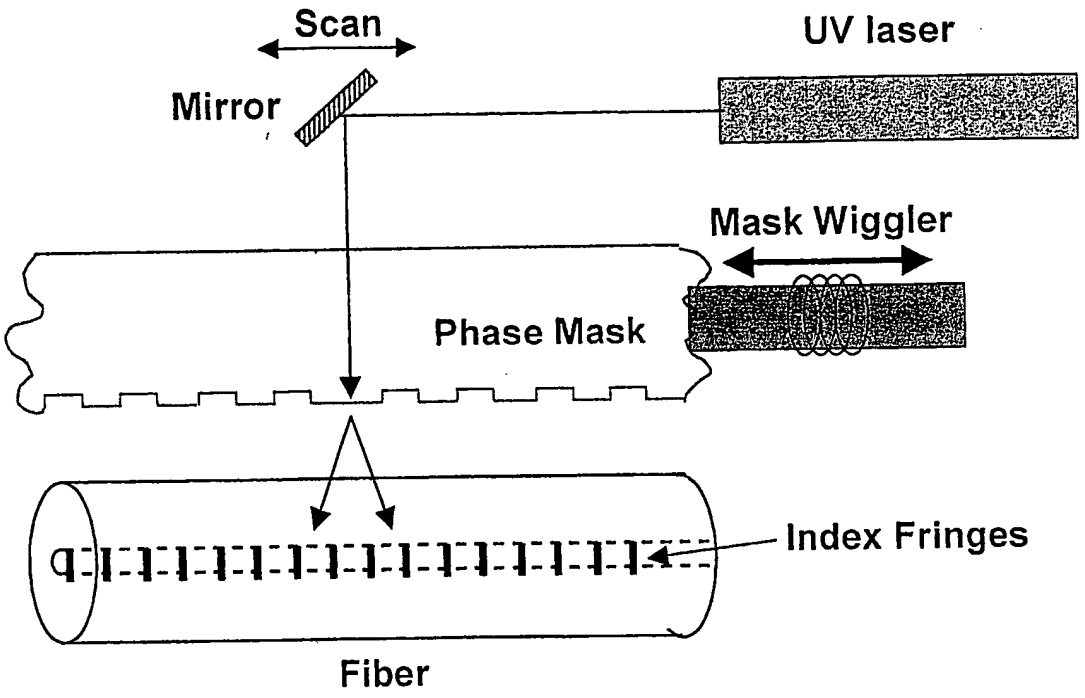

5

Figure 1: Prior Art standard method for writing an FBG by side illumination through a phase mask.

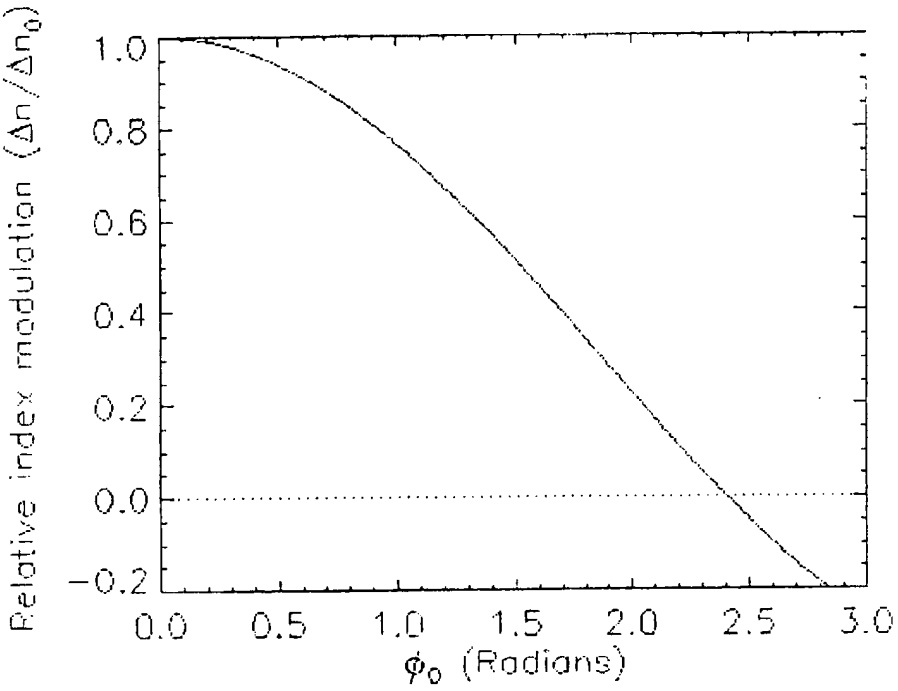

Figure 2: Effective relative modulation amplitude ($\Delta n / \Delta n_0$) of FBG fringes resulting from phase only apodization with sinusoidal phase $\phi_{AP}(x) = \phi_0 \sin(2\pi x / P_A)$ versus the amplitude of the sinusoid ϕ_0.

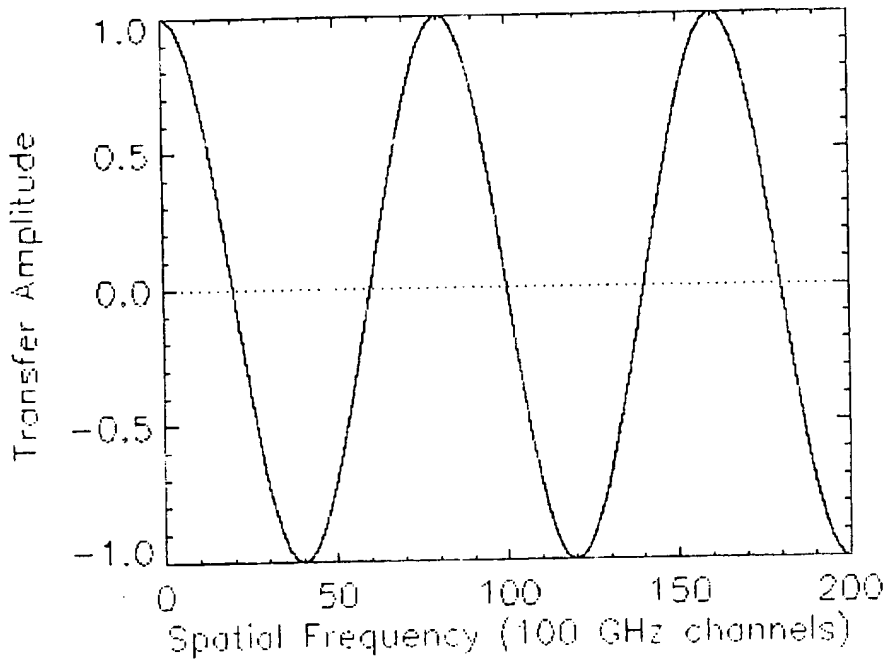

Figure 2(b). Transfer amplitude of sinusoidal phase vs spatial frequency for the case $\Delta x =$ 25 μm.

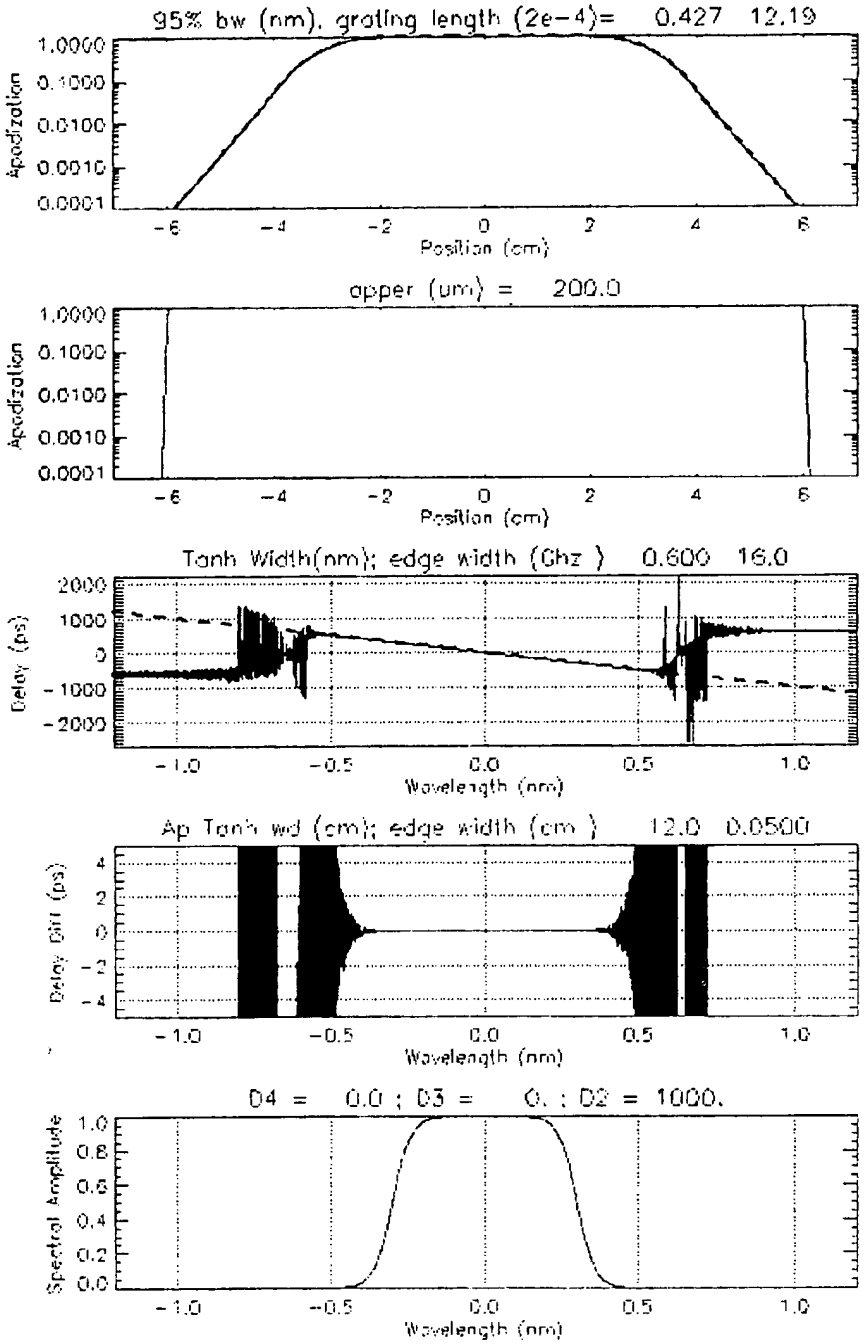

Figure 3: Phase-only apodization of a single channel linearly chirped grating.

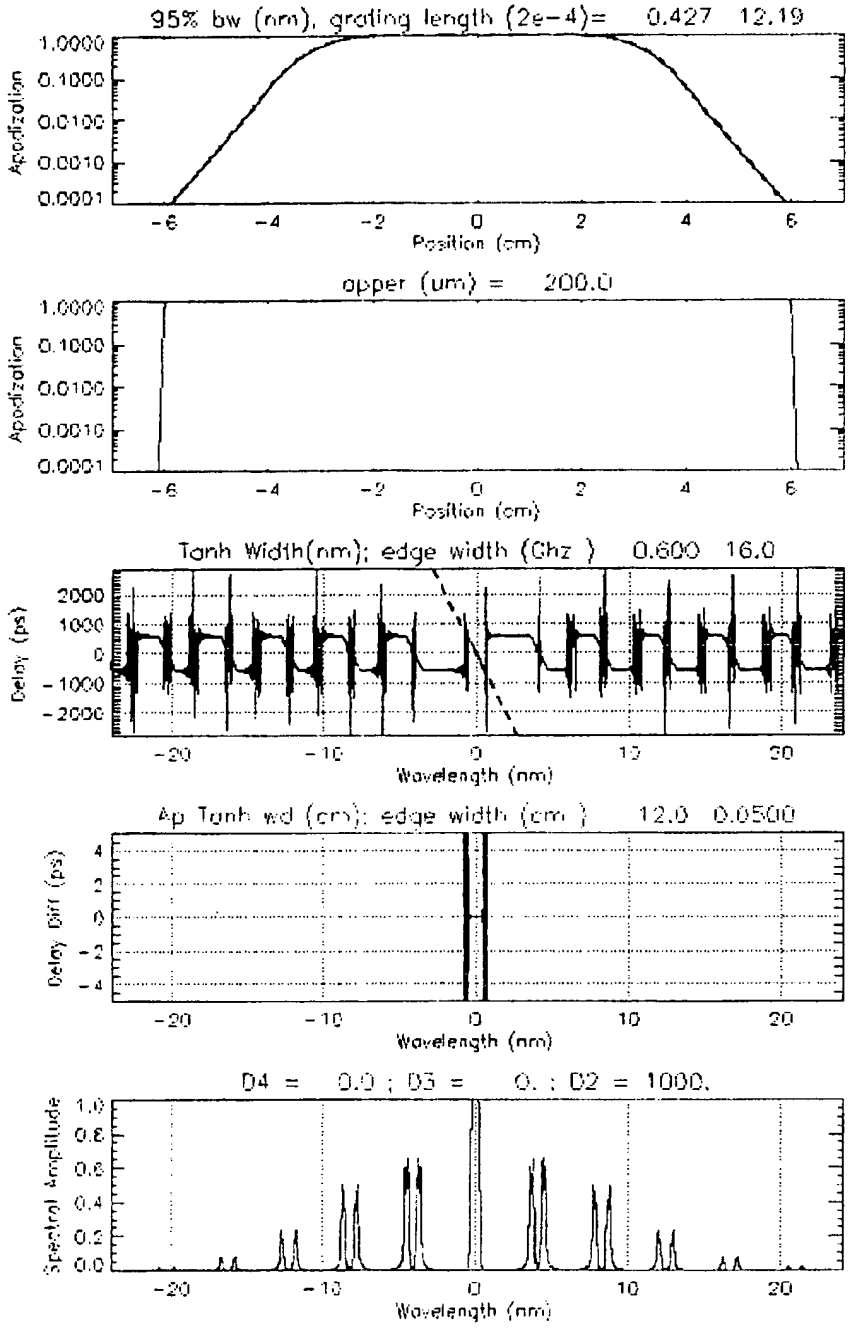

Figure 4A: Phase-only apodization of the same linearly chirped FBG as in Fig. 3. The apodization period is 200 μm.

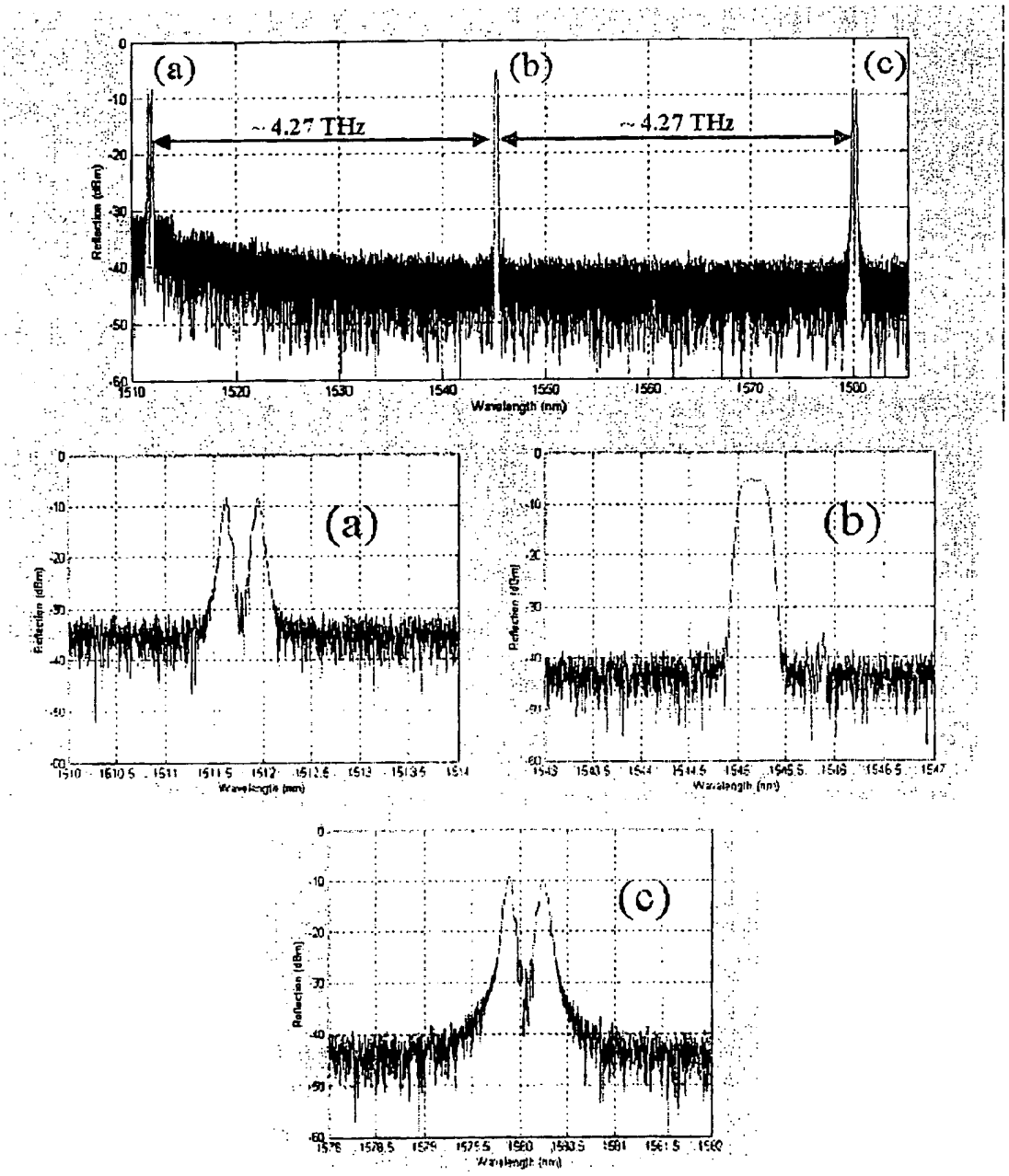

Figure 4B: Experimental demonstration of Phase-only apodization of a linearly chirped (dispersion of ~ -1500 ps/nm) single channel FBG. . The apodization period is about 24 μm.

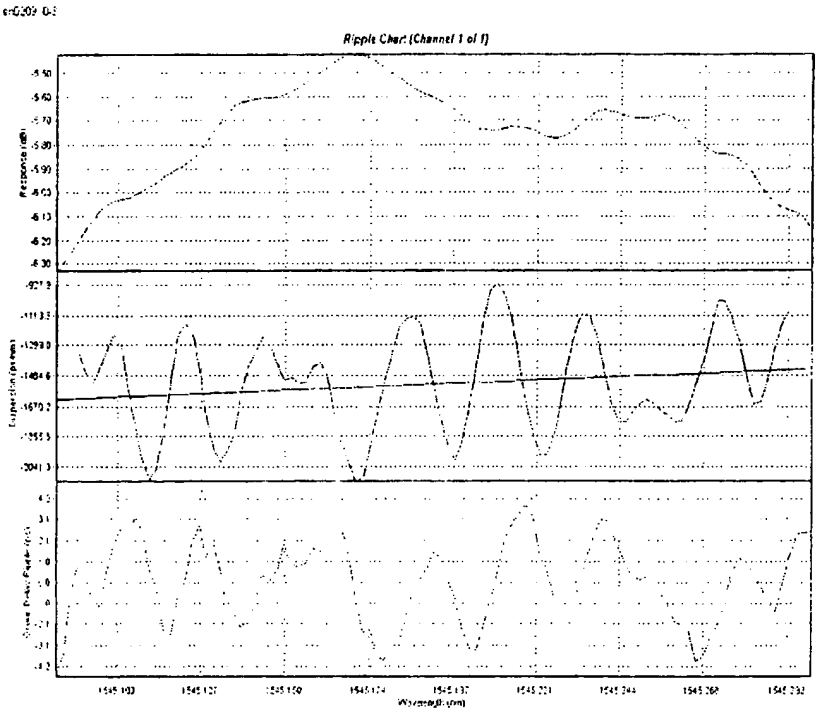

Figure 4C: Experimental demonstration of Phase-only apodization of a linearly-chirped single channel FBG. Measurement of the reflectivity and group delay of the central channel in Fig. 4B shows peak-to-peak group delay variation of less than 8 ps.

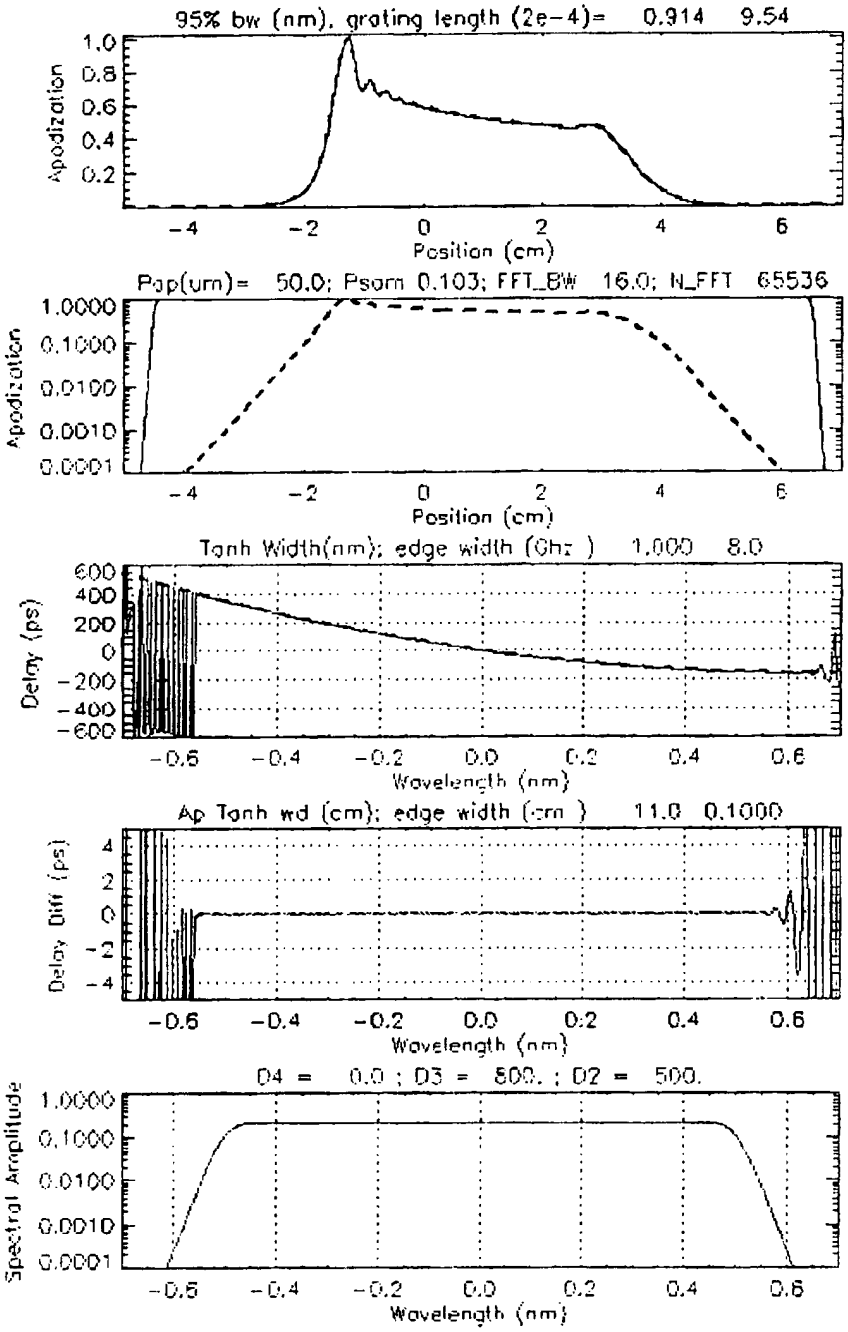

Figure 5: Phase-only apodization of a nonlinearly chirped FBG. Target dispersion is $D = (-500\,ps/nm) + (800\,ps/nm^2)\Delta\lambda$. Phase apodization period is 50 μm.

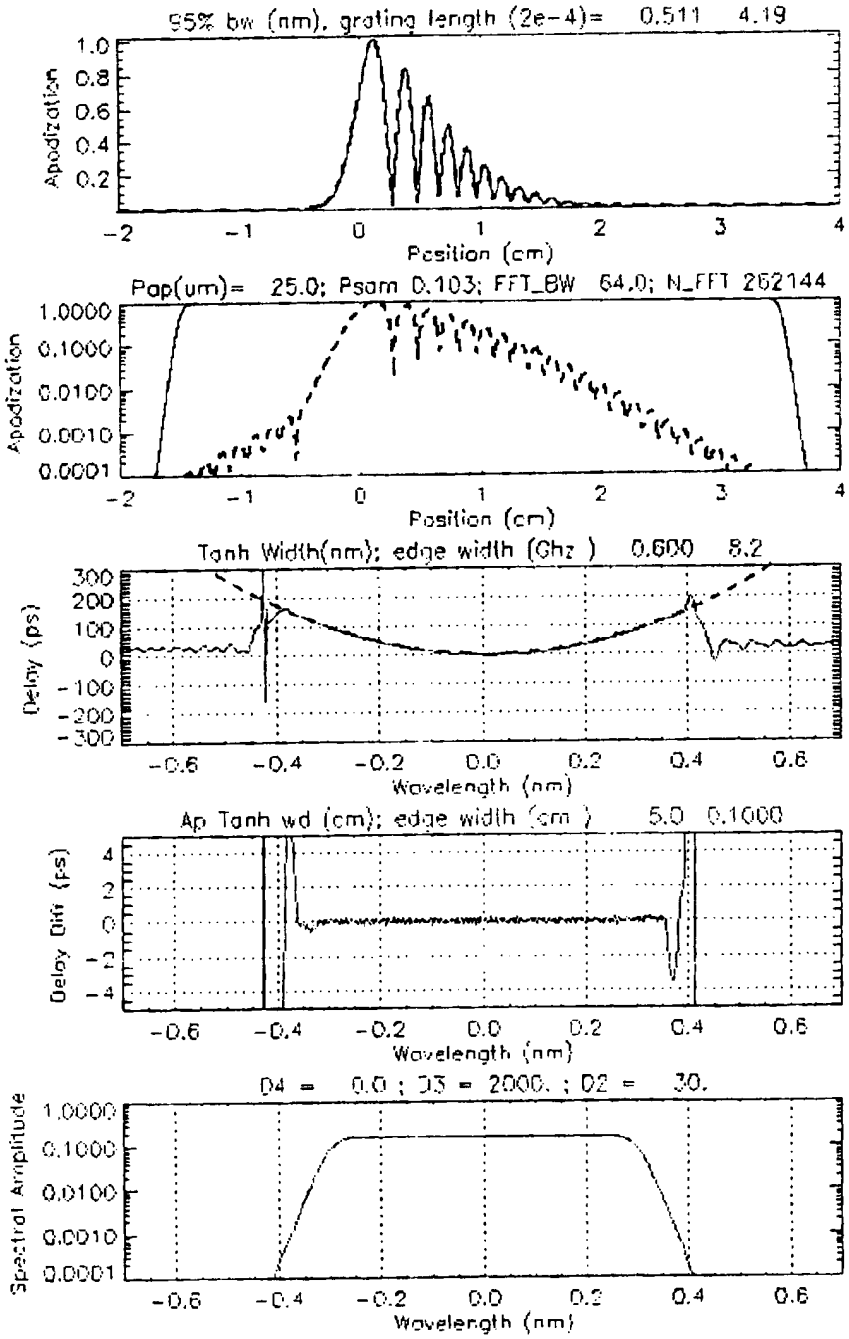

Figure 6: Phase-only apodization of a nonlinearly chirped FBG. Target dispersion is $D = (-30 ps/nm) + (2000 ps/nm^2)\Delta\lambda$. Phase apodization period is 25 μm.

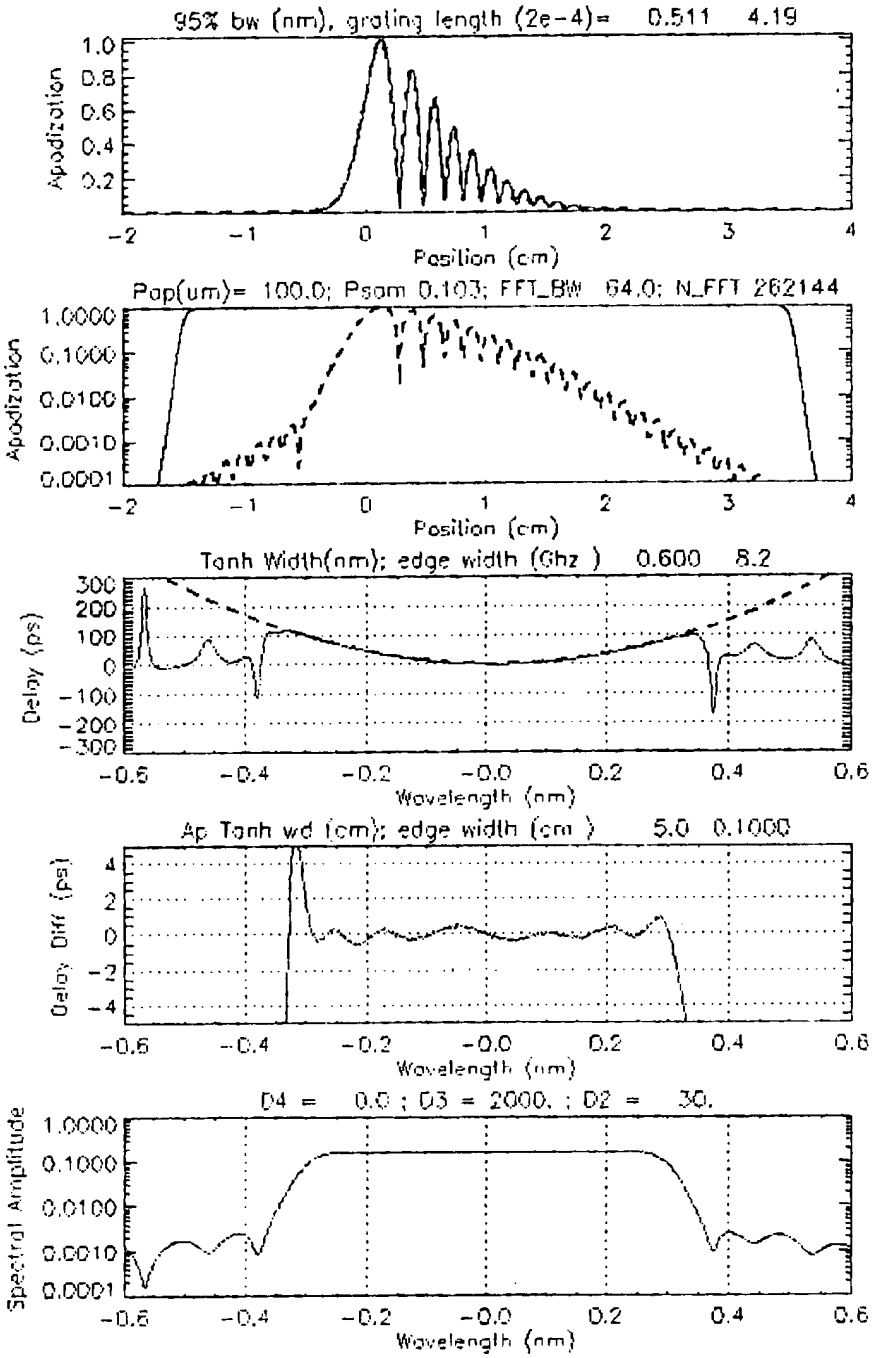

Figure 7: Phase-only apodization of a nonlinearly chirped FBG. Target dispersion is $D = (-30\,ps/nm) \div (2000\,ps/nm^2)\Delta\lambda$. Phase apodization period is 100 μm.

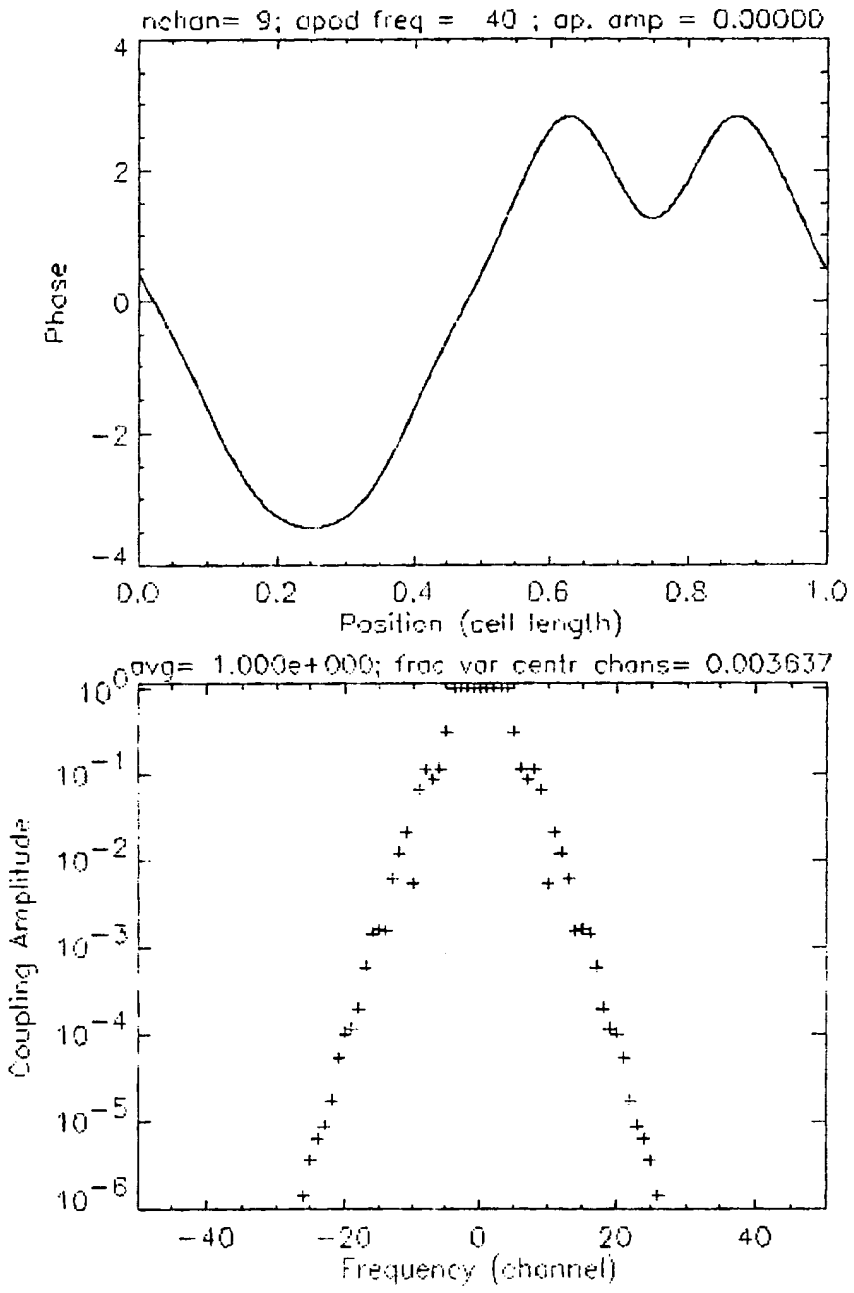

Figure 8: 9-channel phase-only sampling FBG. The top panel shows the periodic phase, which generates the uniform 9 central channels. The bottom panel shows the spectral *amplitude* of the channels generated by the sampling.

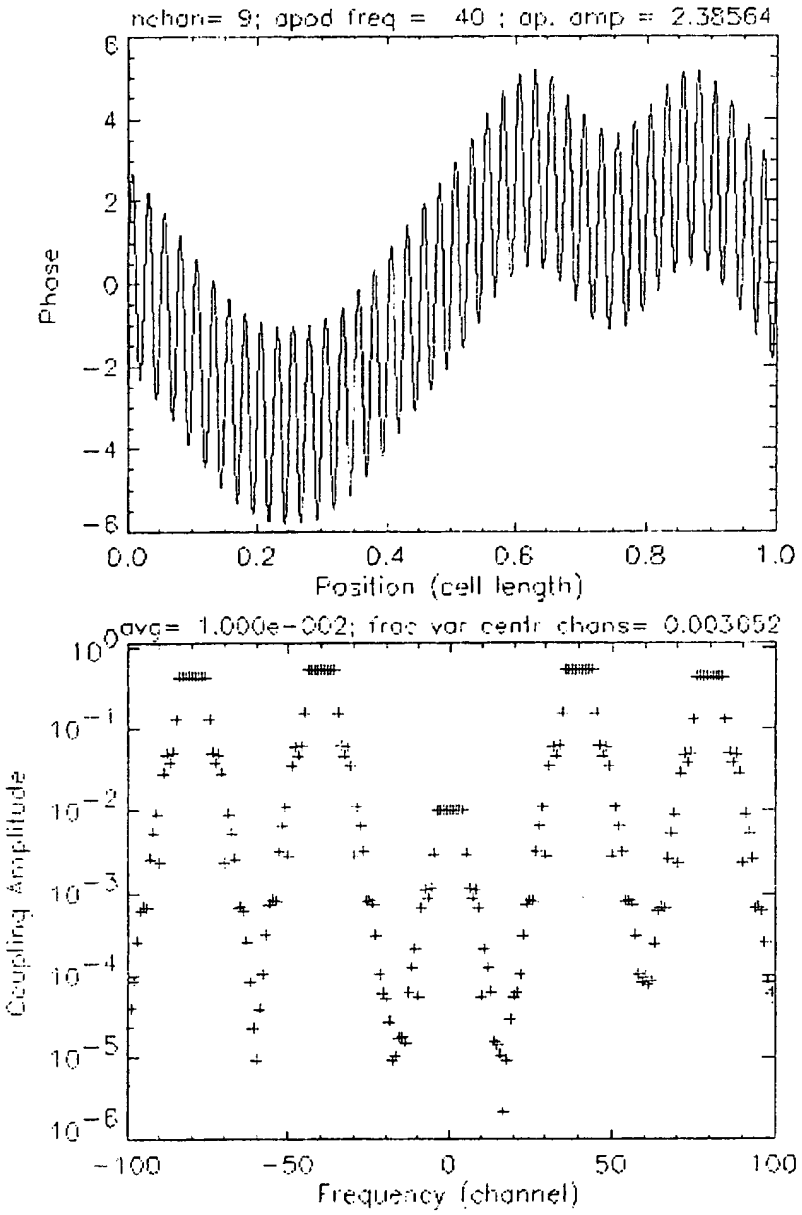

Figure 9: Spectrum of 9-channel phase-only sampling of Fig. 8, which has been modified to include phase-only apodization. The apodization is uniform and reduces all of the 9 center channel amplitudes to 10^{-2} of the maximum. The top panel shows the sum of the sampling and apodization phase (period of ~ 25 μm and amplitude of ±2.3856 rad) which generates spurious 'apodization channels' centered at $\pm 40m$ channels (m =1,2, etc) from the overall center.

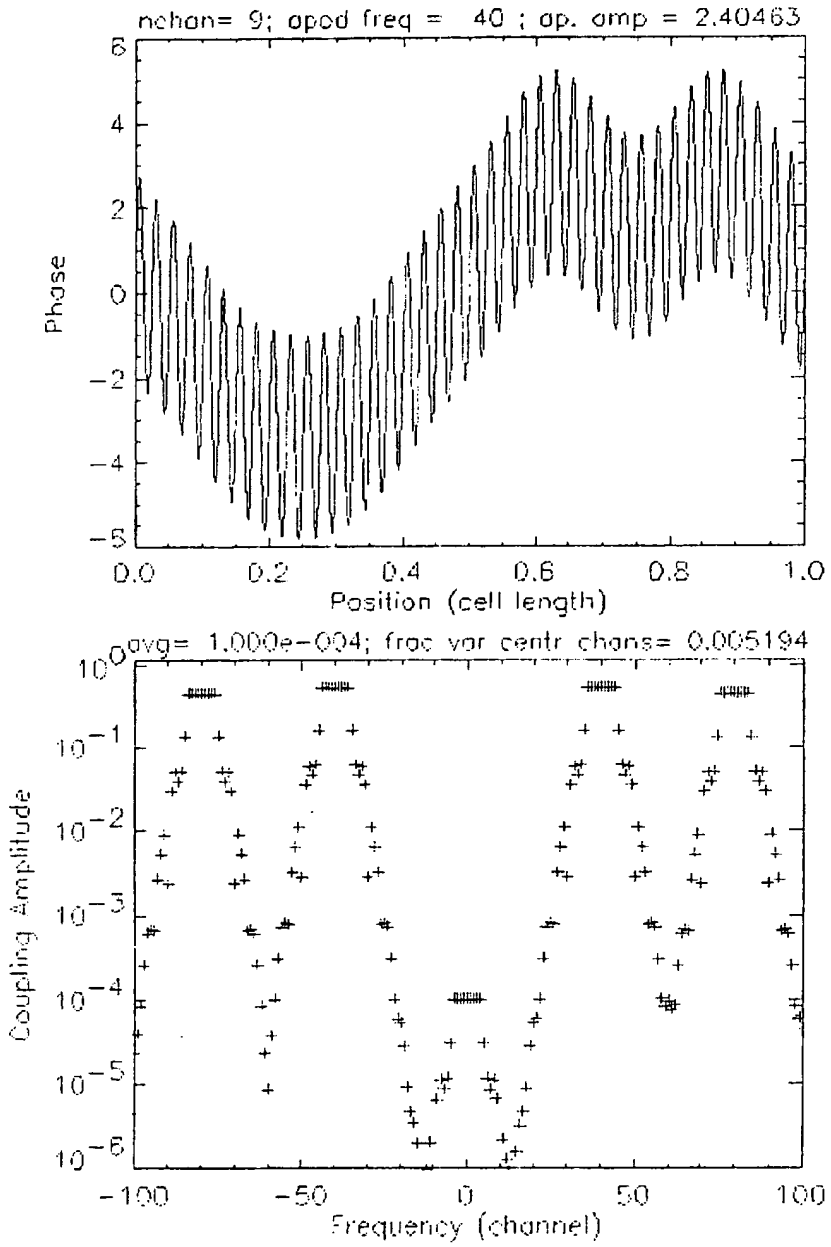

Figure 10: Spectrum of 9 channel phase-only sampling FBG, which has been modified to include phase-only sinusoidal apodization. The apodization is uniform (period of ~ 25 μm and amplitude of ±2.4046 rad) and reduces the center 9 channel amplitudes to 1×10^{-4} of the maximum.

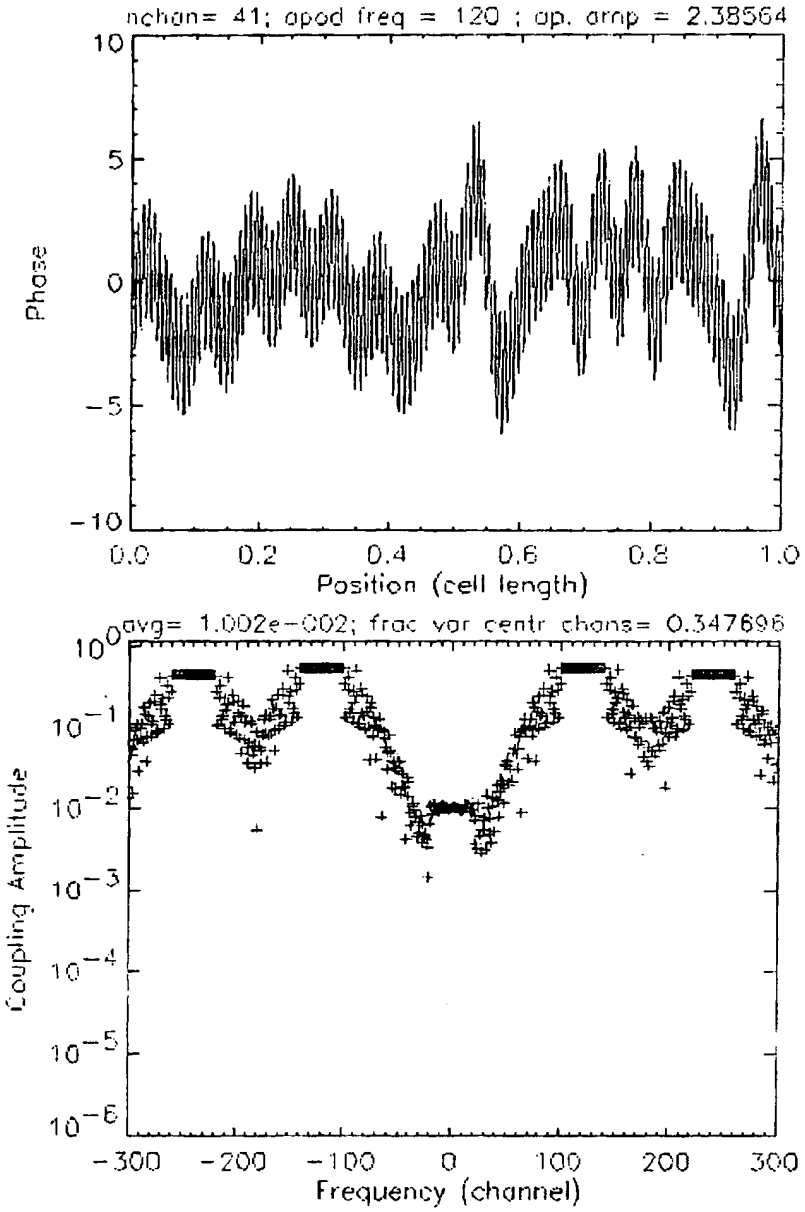

Figure 11: Spectrum of 41-channel FBG with phase-only sampling and apodization. The apodization is uniform (period of ~ 8.3 μm and amplitude of ±2.386 rad) which generates spurious 'apodization channels' at ~ ±124*m* channels (*m* =1,2, etc) from the center. The target amplitude is 10^{-2} of the maximum, but, because the spurious channels are too close to the center channels, significant nonuniformity generated by interference is observed.

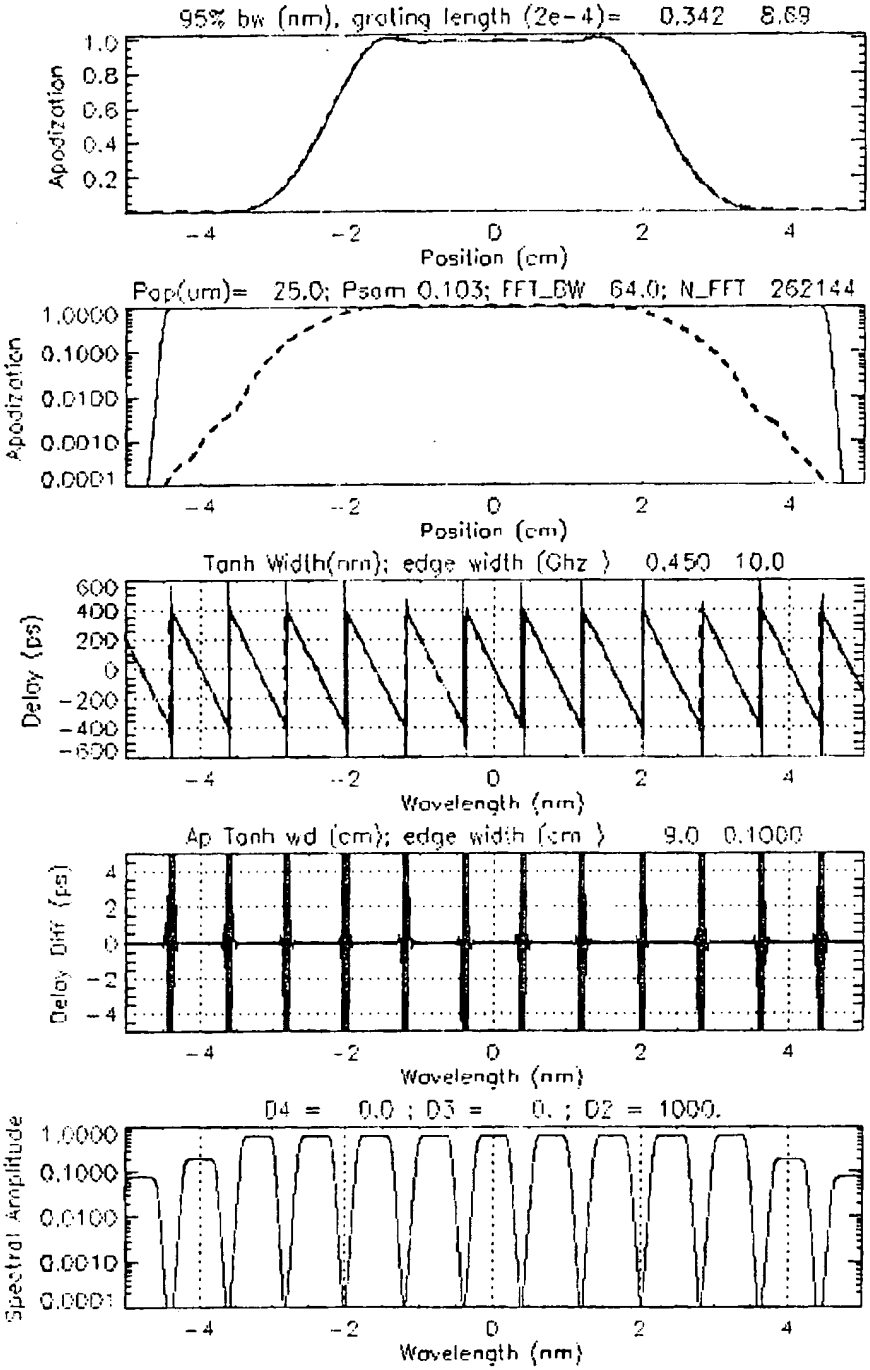

Figure 12: 9 channel linearly chirped (D = -1000 ps/nm) phase-only sampled FBG, which has been phase-only apodized (apodization period of 25 μm).

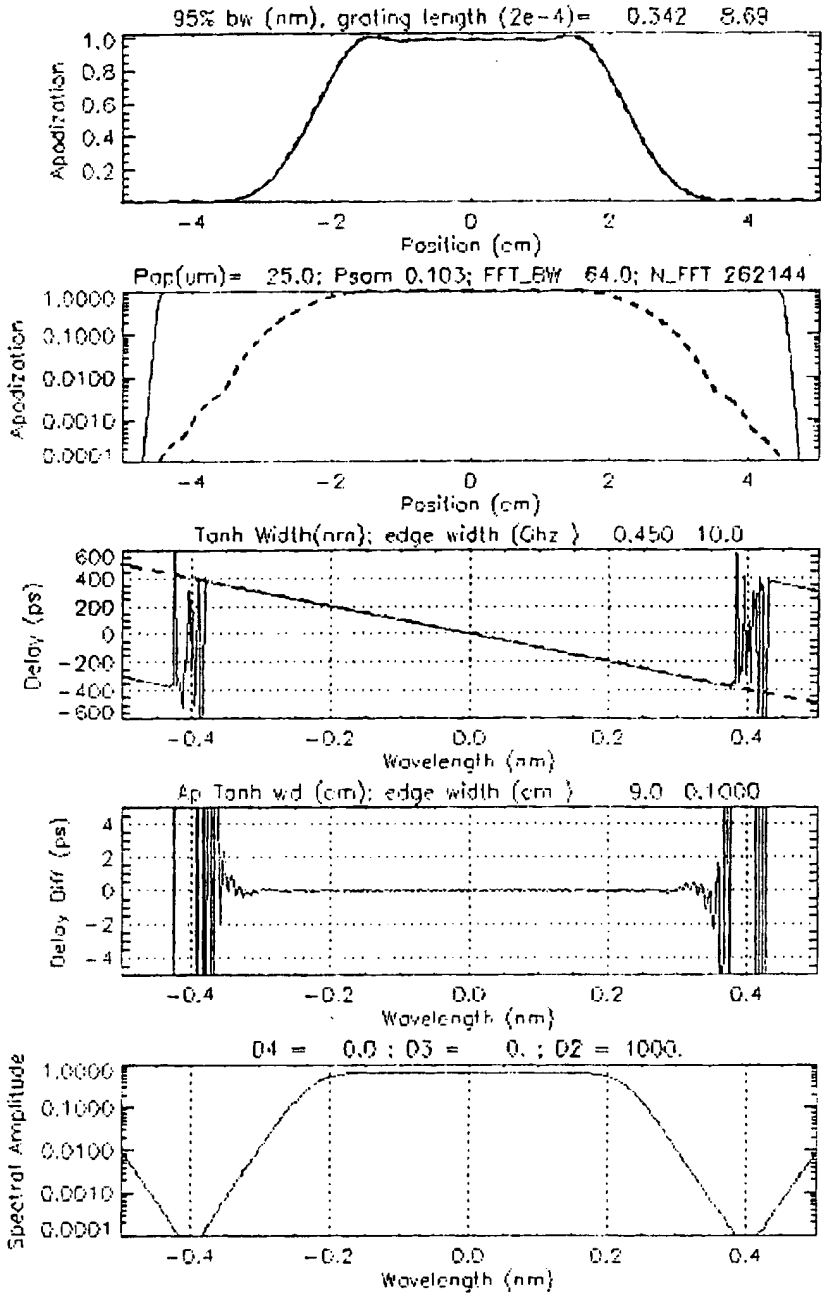

Figure 13: Central channel of 9-channel linearly chirped (D = -1000 ps/nm) phase-only sampled FBG, which has been phase-only apodized (apodization period of 25 μm). The deviation from the desired linear group delay is negligible over the designed bandwidth of the channel.

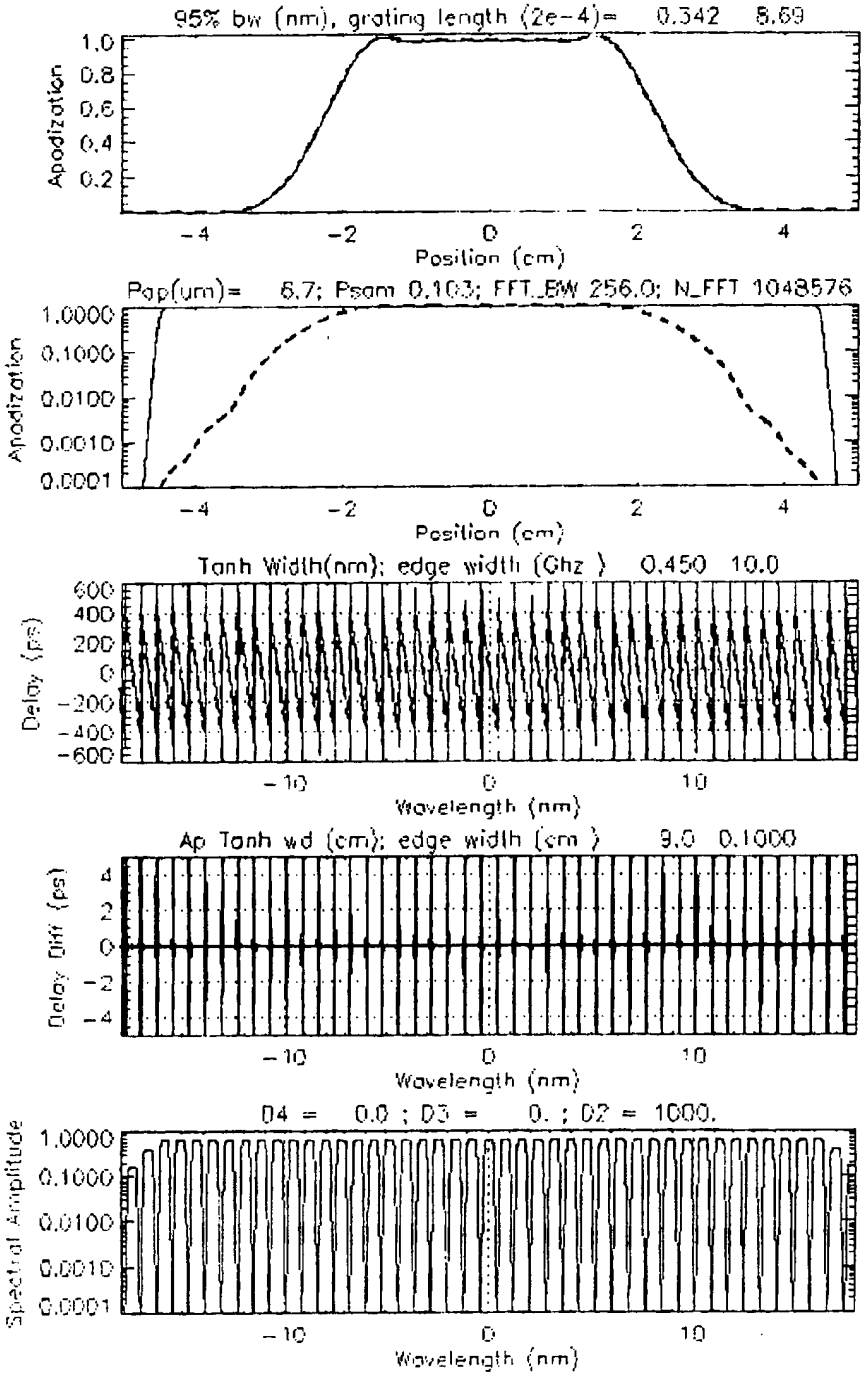

Figure 14: 41 channel linearly chirped (D = -1000 ps/nm) phase-only sampled FBG. which has been phase-only apodized (apodization period of ~ 6.7 μm).

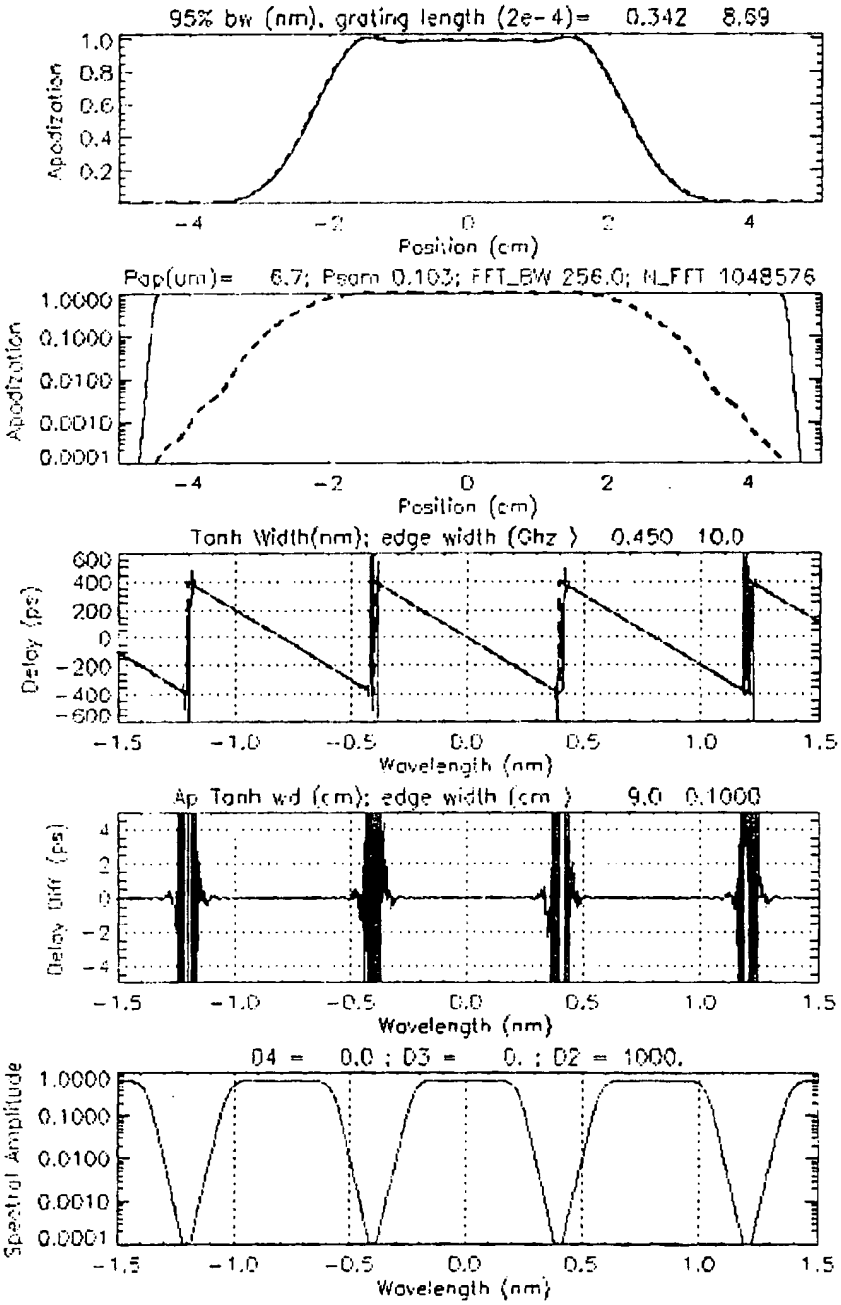

Figure 15: Central channels of 41-channel linearly chirped (D = 1000 ps/nm) phase-only sampled FBG, which has been phase-only apodized (apodization period of ~ 6.7 μm). The deviation from the desired linear group delay is negligible over the designed bandwidth of the channels.